

## RESEARCH ARTICLE

# A novel high-affinity inhibitor against the human ATP-sensitive Kir6.2 channel

Yajamana Ramu\*, Yanping Xu\*, and Zhe Lu 

The adenosine triphosphate (ATP)-sensitive ( $K_{ATP}$ ) channels in pancreatic  $\beta$  cells couple the blood glucose level to insulin secretion.  $K_{ATP}$  channels in pancreatic  $\beta$  cells comprise the pore-forming Kir6.2 and the modulatory sulfonylurea receptor 1 (SUR1) subunits. Currently, there is no high-affinity and relatively specific inhibitor for the Kir6.2 pore. The importance of developing such inhibitors is twofold. First, in many cases, the lack of such an inhibitor precludes an unambiguous determination of the Kir6.2's role in certain physiological and pathological processes. This problem is exacerbated because Kir6.2 knockout mice do not yield the expected phenotypes of hyperinsulinemia and hypoglycemia, which in part, may reflect developmental adaptation. Second, mutations in Kir6.2 or SUR1 that increase the  $K_{ATP}$  current cause permanent neonatal diabetes mellitus (PNDM). Many patients who have PNDM have been successfully treated with sulphonylureas, a common class of antidiabetic drugs that bind to SUR1 and indirectly inhibit Kir6.2, thereby promoting insulin secretion. However, some PNDM-causing mutations render  $K_{ATP}$  channels insensitive to sulphonylureas. Conceptually, because these mutations are located intracellularly, an inhibitor blocking the Kir6.2 pore from the extracellular side might provide another approach to this problem. Here, by screening the venoms from >200 animals against human Kir6.2 coexpressed with SUR1, we discovered a small protein of 54 residues (SpTx-1) that inhibits the  $K_{ATP}$  channel from the extracellular side. It inhibits the channel with a dissociation constant value of 15 nM in a relatively specific manner and with an apparent one-to-one stoichiometry. SpTx-1 evidently inhibits the channel by primarily targeting Kir6.2 rather than SUR1; it inhibits not only wild-type Kir6.2 coexpressed with SUR1 but also a Kir6.2 mutant expressed without SUR1. Importantly, SpTx-1 suppresses both sulfonylurea-sensitive and -insensitive, PNDM-causing Kir6.2 mutants. Thus, it will be a valuable tool to investigate the channel's physiological and biophysical properties and to test a new strategy for treating sulfonylurea-resistant PNDM.

## Introduction

Diabetes is a group of diseases of differing causes (American Diabetes Association, 2011). Among them, permanent neonatal diabetes mellitus (PNDM) was traditionally considered a less common variant of type 1 diabetes mellitus. PNDM has been treated with insulin therapy until about a decade ago when it was discovered to be a monogenic disorder, where gain-of-function mutations of ATP-sensitive  $K^+$  ( $K_{ATP}$ ) channels in pancreatic  $\beta$  cells are the most common cause (Gloyn et al., 2004). This discovery was anticipated by Koster et al. (2000) in their experimental demonstration in mice that the expression of mutant Kir6.2 with gain-of-function mutations caused hypoinsulinemia and hyperglycemia. Subsequently, this finding was further demonstrated in mice with a PNDM-causing mutant Kir6.2 (Girard et al., 2009).

$K_{ATP}$  channels were originally discovered in cardiac myocytes (Noma, 1983). It was subsequently found that extracellular glucose and intracellular ATP inhibit  $K_{ATP}$  channels in pancreatic  $\beta$  cells (Ashcroft et al., 1984; Rorsman and Trube, 1985). This ATP sensitivity enables the channels to play a very critical role in

coupling insulin secretion in pancreatic  $\beta$  cells to blood glucose levels (Nichols, 2006; Ashcroft and Rorsman, 2012, 2013). Elevated blood glucose increases  $\beta$ -cell metabolism, which in turn increases the intracellular ATP level. A higher ATP concentration suppresses  $K_{ATP}$  activity, depolarizing the cell membrane and thereby increasing voltage-gated  $Ca^{2+}$  channel ( $Ca_V$ ) activity. The  $Ca_V$ -mediated  $Ca^{2+}$  influx raises  $[Ca^{2+}]_{in}$ , which in turn triggers insulin release. Individual  $K_{ATP}$  channels in pancreatic  $\beta$  cells are typically formed by the pore-forming unit (Kir6.2) and the modulatory unit sulfonylurea receptor (SUR1; Aguilar-Bryan et al., 1995; Inagaki et al., 1995). The antidiabetic drug sulphonylureas promotes insulin release by binding to SUR1 and thereby inhibiting  $K_{ATP}$  activity. PNDM-causing mutations may occur in either Kir6.2 or SUR1. Thus far, a large fraction of PNDM patients with mutations in Kir6.2 or SUR1 have been successfully treated with sulphonylureas (in lieu of the traditional insulin therapy), although much higher doses are required to treat PNDM, compared with treating type 2 diabetes mellitus (Pearson et al., 2006). This requirement stems from the

Department of Physiology, Perelman School of Medicine, University of Pennsylvania, Philadelphia, PA.

\*Y. Ramu and Y. Xu contributed equally to this work; Correspondence to Zhe Lu: [zhelu@penmedicine.upenn.edu](mailto:zhelu@penmedicine.upenn.edu).

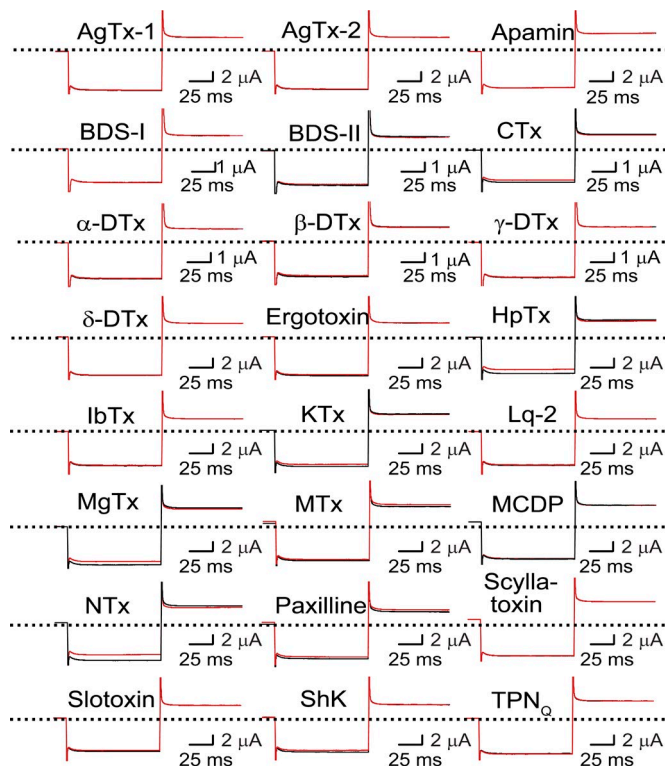


**Figure 1. Relative insensitivity of Kir6.2 to numerous known inhibitors for various types of K<sup>+</sup> channels.** Currents of Kir6.2 coexpressed with SUR1, recorded in 100 mM KCl-containing bath solution without (black traces) or with (red traces) the presence of 24 known K<sup>+</sup> channel inhibitors (1 μM): agitoxin-1 (AgTx-1), agitoxin-2 (AgTx-2), apamin, blood depressing substance I (BDS-I), blood depressing substance II (BDS-II), chlorotoxin (CTx), α-dendrotoxin (α-DTx), β-dendrotoxin (β-DTx), gamma-dendrotoxin (γ-DTx), delta-dendrotoxin (δ-DTx), ergotoxin, heteropodatoxin (HpTx), iberiotoxin (IbTx), kaliotoxin (KTx), *Leiurus quinquestriatus* toxin 2 (Lq-2), margatoxin (MgTx), maurotoxin (MTx), mast cell degranulating peptide (MCDP), noxiustoxin (NTx), paxilline, scyllatoxin, slotoxin, stichodactyla toxin (ShK), and tertiapin-Q (TPN<sub>Q</sub>). In most cases, the pair of compared traces are superimposed. The currents were activated with 3 mM azide (Gribble et al., 1997) and elicited by stepping voltages from the holding potential 0 mV to -80 and then 80 mV before returning to 0 mV. The dotted lines indicate zero-current levels. In a few cases, a very small current occurred at the 0-mV holding potential, which indicates the fact that not all oocytes had an overall reversal potential about ~0 mV in the presence of 100 mM extracellular K<sup>+</sup>.

fact that the gain-of-function mutations almost invariably reduce the effectiveness of sulphonylurea inhibition of K<sub>ATP</sub> current.

Koster et al. (2000) have shown that after a period of sulphonylurea treatment, 30% of PNDM model mice, which expressed a mutant Kir6.2 with gain-of-function mutations, achieved apparent permanent drug-free remission (Remedi et al., 2011). This finding gives the hope that a period of inhibition of K<sub>ATP</sub> channels may lead to permanent remission. Unfortunately, some patients are unresponsive to sulphonylureas, because their mutant channels have such low ATP sensitivity that, at achievable high doses, sulphonylureas cannot adequately lower the elevated K<sub>ATP</sub> activity (Proks et al., 2004, 2013). A different strategy is therefore required to treat these patients, such as directly targeting the Kir6.2 channel. All PNDM-causing mutations in Kir6.2 are located on the cytoplasmic side (Ashcroft, 2005; Remedi and Koster, 2010; Nichols and Remedi, 2012; Ashcroft and Rorsman,

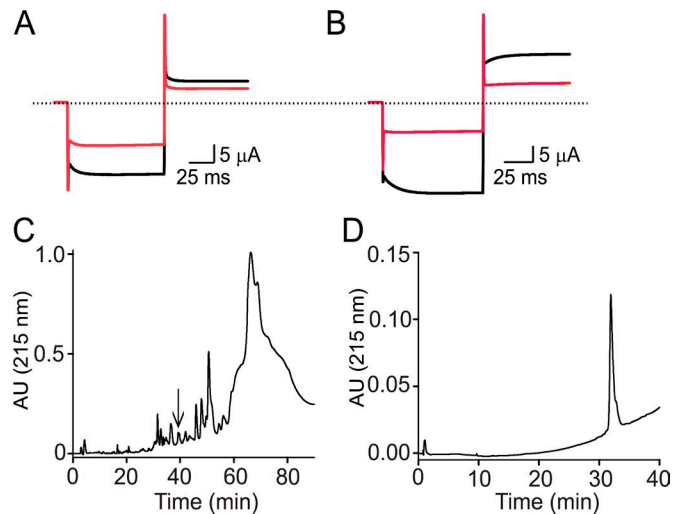


**Figure 2. Purification of an inhibitor against Kir6.2.** (A and B) Currents of Kir6.2 coexpressed with SUR1, recorded in the absence (black trace) or the presence (red trace) of 1:2,000 diluted venom (A) or ~30 nM purified inhibitor from the venom (B). The dotted line indicates the zero-current level. (C) HPLC chromatograph (25-cm-long C18 column) of crude venom, where the sample was eluted with a linear methanol gradient of 1% per min at a 1-ml/min flow rate. The active peak is indicated by the arrow. (D) HPLC chromatograph (15-cm-long C18 column) of the active fraction collected from C, where sample was eluted with a methanol gradient of 0.2% per min at a 0.2-ml/min flow rate.

2013). These mutations, and those in SUR1, may not markedly affect the binding of an inhibitor that plugs the Kir6.2 pore from the extracellular side. It is noteworthy that Kir6.2-containing K<sub>ATP</sub> channels are also present in the heart. If the notion is correct that cardiac sarcolemmal K<sub>ATP</sub> channels are mostly closed and are not essential under a normal metabolic state (Zhang et al., 2010), then targeting pancreatic Kir6.2 in an attempt to treat diabetes may not adversely affect normal cardiac functions. In any case, a Kir6.2 inhibitor is necessary for experimentally testing whether Kir6.2 itself is indeed a useful target to promote insulin secretion. In addition, in many cases, the lack of a specific inhibitor against the Kir6.2 channel prevents an unambiguous determination of its role in certain physiological and pathological processes. The Kir6.2 knockout mice do not exhibit the expected phenotypes of hyperinsulinemia and hypoglycemia, which may, in part, reflect developmental adaptation (Miki et al., 1998). These reasons motivated us to develop a relatively selective Kir6.2 inhibitor.

## Materials and methods

### Biochemistry of an inhibitor against Kir6.2

The venom of *Scolopendra polymorpha* (Spider Pharm) was first fractionated on a 25-cm-long reversed-phase C18 HPLC column (Fig. 2 C). The sample was eluted with a linear methanol gradient (1% per min) by decreasing the water-based mobile and increasing the methanol phase; the flow rate was 1 ml/min. The identified active fraction was then loaded on to a 15-cm-long C18 column eluted with a shallower methanol gradient (0.2% per min); the flow rate was 0.2 ml/min (Fig. 2 D). Mass spectrometry was performed at the Wistar Institute (Philadelphia, PA)

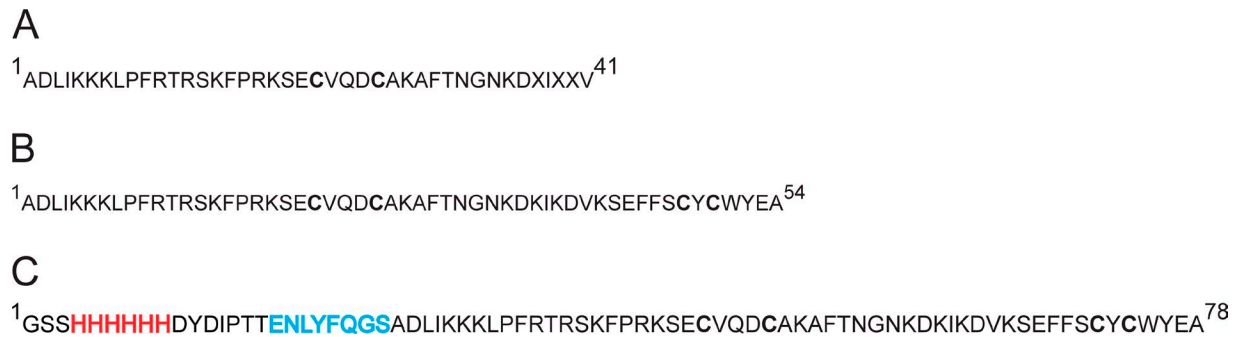


Figure 3. **Amino acid sequence of SpTx-1.** The partial sequence of the purified inhibitor obtained from Edman degradation (A; each letter X indicates an ambiguous residue type that was subsequently determined to be the corresponding one shown in B), the full sequence deduced from cDNA sequencing (B), and the sequence with an extra N-terminal segment containing a 6-His-tag followed by a spacer sequence and then by the cleaving site of the protease TEV (C), where the His-tag and the TEV-cleaving sequence were colored maroon and cyan, respectively.

proteomics facility on an ABI/PerSeptive Voyager DE-PRO MALDI-TOF instrument in positive-ion mode. Samples were spotted to plates coated by using  $\alpha$ -cyano-4-cinnamic acid matrix (Sigma Aldrich) at a concentration of 10 mg/ml. External calibration was performed before the sample analysis. The mass of the purified Kir6.2-inhibiting material, determined on MALDI-TOF, was 6366.6 D. The sequence of the N-terminal 41 residues (except for three ambiguous ones at positions 37, 39, and 40), shown in Fig. 3 A, was identified by Edman degradation at the William Keck facility of Yale University (New Haven, CT).

The full amino acid sequence of the inhibitor against Kir6.2 was deduced from its cDNA sequencing as described below. The total mRNAs were extracted from the venom glands by using TRIzol (Ambion); their cDNAs were produced by using the SuperScript plasmid system (Invitrogen). The cDNA corresponding to the purified inhibitor protein was amplified by PCR, where the 5' end is primed with degenerate oligonucleotides corresponding to the N-terminal amino acid sequence of the inhibitor protein, whereas the 3' end is primed with a poly-A oligonucleotide. From the sequence of the resulting PCR product, we were able to deduce a 54-residue peptide sequence shown in Fig. 3 B.

The peptide of the inhibitor was synthesized with a peptide synthesizer at the William Keck facility of Yale University. To fold the synthetic peptide, we dissolved it in a solution containing 1 mM dithiothreitol and 10 mM Tris (pH 8.0). 24–48 h later when dithiothreitol became oxidized and disulfide bonds were presumably formed (on the basis of the expected retention time on HPLC), the inhibitor in the correct conformation was purified with a reversed-phase C18 column. The recombinant version of the inhibitor was produced through an *Escherichia coli* expression system. An N-terminal 6-His and a specific protease-cutting sequence were added for affinity purification with a Co<sup>2+</sup> column and a subsequent cleavage of the His-tag with the tobacco etch virus (TEV) protease, respectively. Cell lysate (50 ml from 1 liter culture) was loaded onto a Co<sup>2+</sup>-affinity column, which was washed and eluted with PBS solutions containing 20 mM and 500 mM imidazole, respectively. The eluted sample was purified by HPLC. When desirable, the His-tag was cleaved, before HPLC purification, with recombinant TEV protease (produced in house) in a solution containing 50 mM Tris-HCl (pH 8.0), 0.5 mM EDTA, 3 mM reduced glutathione, and 0.3 mM oxidized glutathione; the

ratio between TEV and inhibitor was 1:100 in absorbance unit at 280 nm. All purified inhibitors were stored at –20°C.

### Mutagenesis and electric recordings of K<sub>ATP</sub> channels

The mutant Kir6.2 channel cDNAs were produced through PCR-based mutagenesis and were confirmed with DNA sequencing. Kir1.1 cDNA was provided by K. Ho (Washington University School of Medicine, St. Louis, MO) and S. Herbert (Yale University, New Haven, CT). Kir2.1, Kir3.1, Kir6.1, Kir6.2, and SUR1 cDNAs were provided by L. Jan (University of California, San Francisco, CA). Kir3.2 cDNA was provided by H. Lester (California Institute of Technology, Pasadena, CA). Kir3.4 cDNA was provided by D. Clapham (Harvard University, Boston, MA). Kir4.1 cDNA was provided by R. Buono (University of Pennsylvania, Philadelphia, PA) and T. Ferraro (Baylor College of Medicine, Houston, TX). M2 cDNA was provided by E.G. Peralta (Harvard University, Boston, MA), and TEV cDNA was provided by G. D. Van Duyne (University of Pennsylvania, Philadelphia, PA). The complementary RNAs of Kir channels, SUR1, and the muscarinic type 2 (M2) receptor were synthesized with T7 polymerase using the corresponding linearized cDNAs as templates. Channel currents were recorded from *Xenopus laevis* oocytes, which were injected with complementary RNA encoding specific Kir channels and other necessary components by using a two-electrode voltage-clamp amplifier (Oocyte Clamp OC-725C; Warner Instruments Corp.; Jin and Lu, 1998). The resistance of electrodes filled with 3 M KCl were 0.2–0.4 MΩ. To elicit current through the channel, the membrane potential of oocytes was stepped from the holding potential of 0 mV to –80 mV then to +80 mV before returning back to 0 mV. The bath solution contained 100 mM KCl, 0.3 mM CaCl<sub>2</sub>, 1.0 mM MgCl<sub>2</sub>, and 10 mM HEPES, pH 7.6. Kir6.1 and Kir6.2 channels, coexpressed with SUR1, were activated after ~5 min exposure to 3 mM azide. Kir3.1/3.2 and Kir3.1/3.4 channels were coexpressed with the M2 receptor and activated with 150 μM acetylcholine. The inhibitor concentrations were calculated by using an extinction coefficient 8.7 mM<sup>–1</sup> cm<sup>–1</sup> (for synthetic and recombinant versions) or 11.7 mM<sup>–1</sup> cm<sup>–1</sup> (for the recombinant version with the extra sequence shown in Fig. 3 C) at 280-nm wavelength. The inhibitor against Kir6.2 used in the study was purified native, synthetic, or recombinant protein, as specified. All other existing inhibitors were either made recombinantly in house or purchased from Alomone Labs (Kit EK300). The

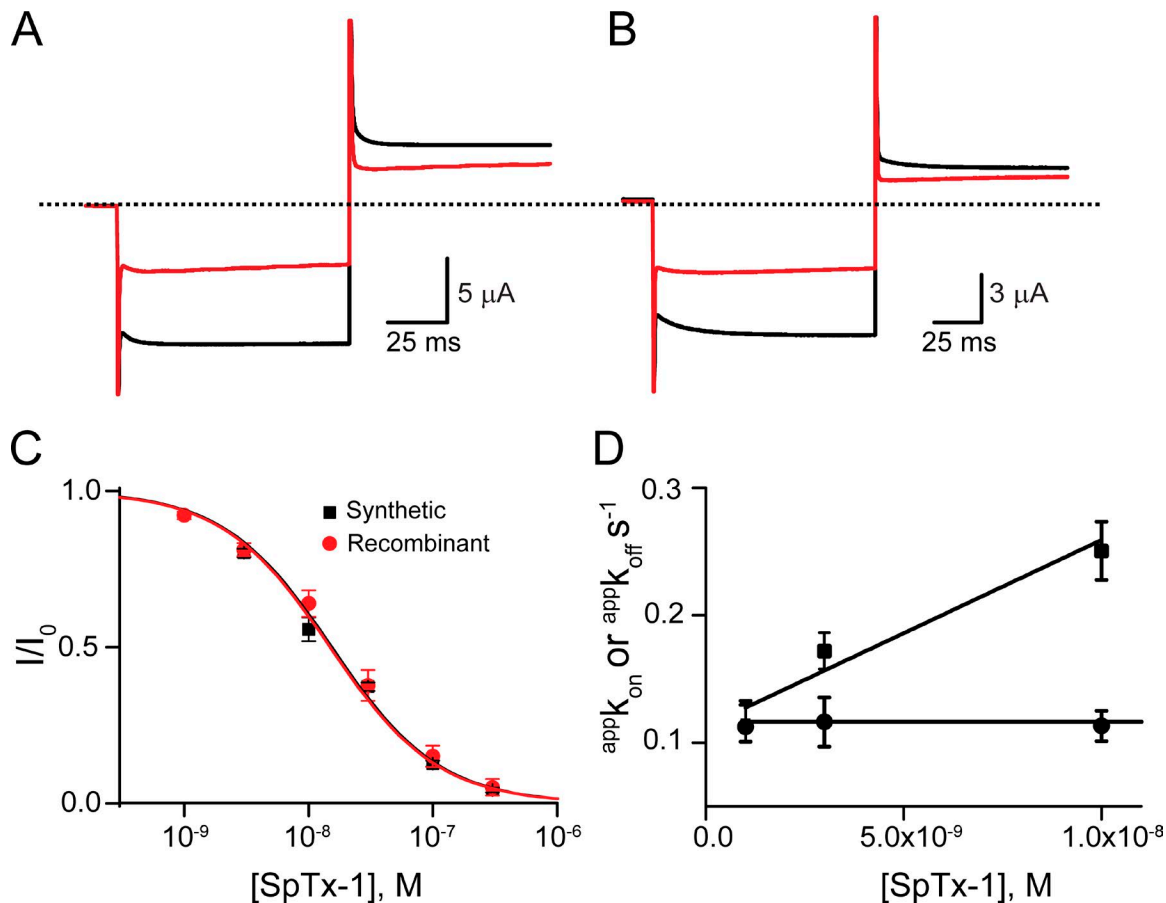


Figure 4. **Properties of synthetic and recombinant SpTx-1.** (A and B) Currents of Kir6.2 coexpressed with SUR1, recorded in the absence (black trace) or presence (red trace) of 20 nM synthetic (A) and recombinant (B) SpTx-1. The dotted line indicates the zero-current level. (C) Fractions of currents plotted against the concentration of synthetic or recombinant SpTx-1. The curves superimposed on data correspond to the fits of an equation for a bimolecular reaction. The fitted  $K_d$  values are  $(1.53 \pm 0.13) \times 10^{-8}$  M ( $n = 6$ , synthetic) and  $(1.48 \pm 0.12) \times 10^{-8}$  M ( $n = 6$ , recombinant). (D)  $appk_{on}$  (solid squares) and  $appk_{off}$  (solid circles) of current inhibition plotted against the concentration of recombinant SpTx-1 with the extra sequence shown in Fig 3 C. A linear fit yielded  $k_{on}$  of  $(1.46 \pm 0.42) \times 10^7$  M $^{-1}$  s $^{-1}$  ( $n = 5$ ), and  $k_{off}$ , calculated from the mean of  $appk_{off}$  at various SpTx-1 concentrations, was  $(1.23 \pm 0.19) \times 10^{-1}$  s $^{-1}$  ( $n = 5$ ). Data represent the mean  $\pm$  SEM.

screened venoms were either obtained from Spiderpharm, Sigma Aldrich, and Latoxan or provided as gifts. In the screen, individual venom samples (1  $\mu$ l) were manually pipetted into a recording chamber (100  $\mu$ l). In the kinetic study, a recording chamber (1 ml) was perfused with a basic homemade gravity-based system where the dead time of solution exchange is  $\sim$ 1 sec.

#### Data analysis

All data were analyzed by using Origin 8 (OriginLab) and are presented as mean  $\pm$  SEM of  $n$  experiments.

## Results

### Screening for inhibitory activity against the human $K_{ATP}$ channel

We searched for inhibitory activity against the  $K_{ATP}$  channels formed by human Kir6.2 and SUR1, which were heterologously expressed in *X. laevis* oocytes. We first tested 24 reagents, each of which is known to inhibit certain types of  $K^+$  channel. At 1  $\mu$ M concentration, these inhibitors suppressed little or no  $K_{ATP}$  current (Fig. 1). We next screened venoms from more than 200 poisonous

animals, such as scorpions, snakes, spiders, and centipedes. Among them, we found that only the venom of the centipede *S. polymorpha* contained the inhibitory activity against the  $K_{ATP}$  current. As shown in Fig. 2 A, after addition of the venom to the recording solution in 1:2,000 final dilution, the  $K_{ATP}$  current dropped  $\sim$ 40%.

### Biochemical purification and identification of an inhibitor for the $K_{ATP}$ channel

We purified the inhibitory material by HPLC (Fig. 2). The crude venom was loaded onto a 25-cm-long reversed-phase (C18) column and eluted with a linear methanol gradient (1% per min; Fig. 2 C). We tested each eluted fraction against the  $K_{ATP}$  channels and found that only one resulting fraction, which corresponds to a small peak, contained the  $K_{ATP}$ -inhibiting activity. To evaluate this fraction, we loaded it on 15-cm-long C18 column and eluted it with a shallower methanol gradient (0.2% per min; Fig. 2 D). The chromatograph displays a practically single peak, a feature suggesting that the active material has been highly purified. We found that the eluted fraction, which corresponds to this peak, remained active. After biochemical identification of the active material in a series of studies described below, we estimated the inhibitor concentration

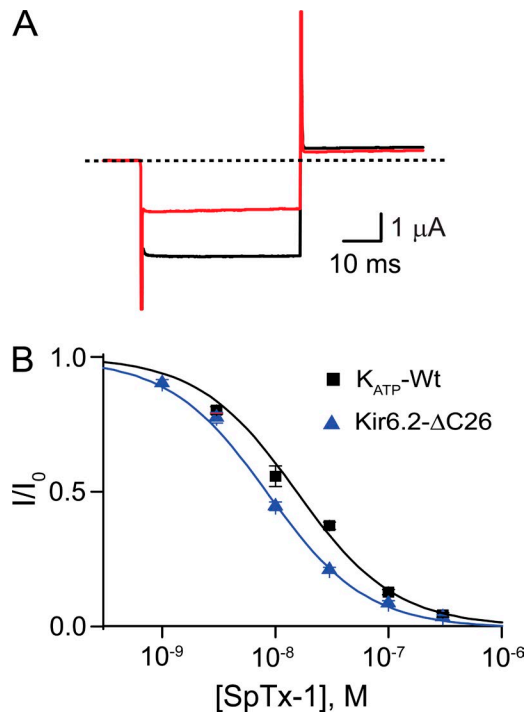


Figure 5. **Inhibition of the Kir6.2-ΔC26 mutant by SpTx-1.** (A) Currents of the Kir6.2-ΔC26 mutant channels, recorded in the absence (black trace) or presence (red trace) of 10 nM synthetic SpTx-1. (B) Fractions of currents, recorded from WT and Kir6.2-ΔC26 mutant channels, are plotted against the concentration of recombinant SpTx-1. The curves superimposed on data correspond to the fits of an equation for a bimolecular reaction. The fitted  $K_d$  values are  $(1.53 \pm 0.13) \times 10^{-8}$  M ( $n = 6$ ) for WT channels and  $(8.52 \pm 0.37) \times 10^{-9}$  M ( $n = 6$ ) for the Kir6.2-ΔC26 mutant channels. Data represent the mean  $\pm$  SEM.

in the final sample solution from its absorbance using an extinction coefficient calculated from its composition (Gill and von Hippel, 1989). At 30 nM, the material inhibited the  $K_{ATP}$  current by more than half (Fig. 2 B). We had a very limited amount (150 μl) of venom at the time and could not purify a sufficient amount of the inhibitory material to both obtain a dose-response curve and perform the necessary biochemical studies. Fortunately, the small amount of purified sample was just barely enough for the following biochemical identification of the inhibitor.

Mass spectrometry revealed that the inhibitor has a mass of 6366.6 D, which suggests that it is a small protein. To obtain its amino acid sequence, we analyzed the purified protein sample by the Edman degradation method. In doing so, we obtained the sequence of its N-terminal 41 residues, except for the three ambiguous ones at positions 37, 39, and 40 (Fig. 3 A). To obtain the remaining C-terminal sequence, we resorted to cDNA sequencing. To do so, we extracted the total mRNAs from the venom glands and generated their cDNAs by means of reverse transcription. The cDNA corresponding to the purified inhibitor protein was enriched through PCR, in which one end was primed with degenerate oligonucleotides corresponding to the N-terminal amino acid sequence of the inhibitory protein, whereas the other end was primed with a poly-A oligonucleotide. From the sequence of the resulting PCR product, we were able to deduce a 54-residue peptide sequence (Fig. 3 B). The sequence of N-terminal 41 residues predicted from the cDNA

matches that of the purified protein already determined from peptide sequencing. The amino acid sequence deduced from the cDNA sequence corresponds to a theoretical mass of 6370 D, which is 4 D greater than the observed mass of the purified inhibitory protein. Notably, the protein sequence contains four cysteines. The difference of 4 D between the observed mass and the theoretical mass is consistent with these cysteines forming two pairs of disulfide bonds.

### Synthesis of the $K_{ATP}$ -inhibiting protein

To verify that this identified protein is indeed the inhibitor, we produced it in two ways. First, we produced the peptide by means of chemical synthesis. After air oxidation, the synthesized material was purified with HPLC. At 20 nM concentration, the purified synthetic protein suppressed the  $K_{ATP}$  current by about half (Fig. 4 A). Second, we made the protein through a bacterial recombination process. Again, at 20 nM, the resulting recombinant protein also inhibits the  $K_{ATP}$  current by about half (Fig. 4 B). Thus, we have indeed obtained an inhibitor against the human  $K_{ATP}$  channels, and as expected, the synthetic and recombinant versions of the inhibitor are practically the same. We named the inhibitor SpTx-1.

### Characterization of SpTx-1

Fig. 4 C shows the fraction of the  $K_{ATP}$  current versus the concentration of the synthetic and recombinant versions of SpTx-1 (Fig. 3 B). Fitting this relation with an equation, which describes a one-to-one inhibitor-channel interaction, yielded an apparent  $K_d$  of 15 nM. The kinetics of the inhibitor-channel interaction is too fast to be accurately determined in our experimental system. However, we serendipitously found that when the N terminus of the inhibitor is attached with an extra segment (Fig. 3 C), this recombinant protein inhibited the channels with comparable apparent  $K_d$  but slower kinetics. The extra N-terminal segment contains a six-histidine sequence for  $\text{Co}^{+}$ -affinity purification followed by a seven-residue spacer sequence and then an eight-residue protease-cutting sequence for removing the histidines (Fig. 3 C). We were able to examine the kinetics of this recombinant inhibitor with the extra segment. Fig. 4 D plots the apparent  $k_{on}$  and  $k_{off}$  ( $^{app}k_{on}$  and  $^{app}k_{off}$ ) of the channel inhibition versus the concentration of SpTx-1. Although  $^{app}k_{on}$  increased linearly with the inhibitor concentration,  $^{app}k_{off}$  remained practically the same. Fitting a linear equation to the relation between  $^{app}k_{on}$  and the inhibitor concentration yielded an apparent  $k_{on}$  of  $(1.46 \pm 0.42) \times 10^7 \text{ M}^{-1} \text{ s}^{-1}$ , whereas the apparent  $k_{off}$ , estimated from the mean  $^{app}k_{off}$ , was  $(1.23 \pm 0.19) \times 10^{-1} \text{ s}^{-1}$ ; the calculated  $K_d$  from the  $k_{off}/k_{on}$  ratio was 8.42 nM.

Next, we checked whether, unlike the antidiabetic drug sulfonylurea, SpTx-1 suppresses the  $K_{ATP}$  current channels by primarily targeting the pore-forming subunit Kir6.2, instead of the modulatory subunit SUR1. To do so, we took advantage of the Kir6.2 mutant that lacks the C-terminal 26 residues, which is dubbed Kir6.2-ΔC26 (Tucker et al., 1997). Unlike WT Kir6.2, this mutant has been shown to form functional channels without coexpression of SUR1. As shown in Fig. 5 A, at 10 nM, the recombinant version of SpTx-1 suppressed the Kir6.2-ΔC26 current by about half. Analyzing the dose-response curve yielded

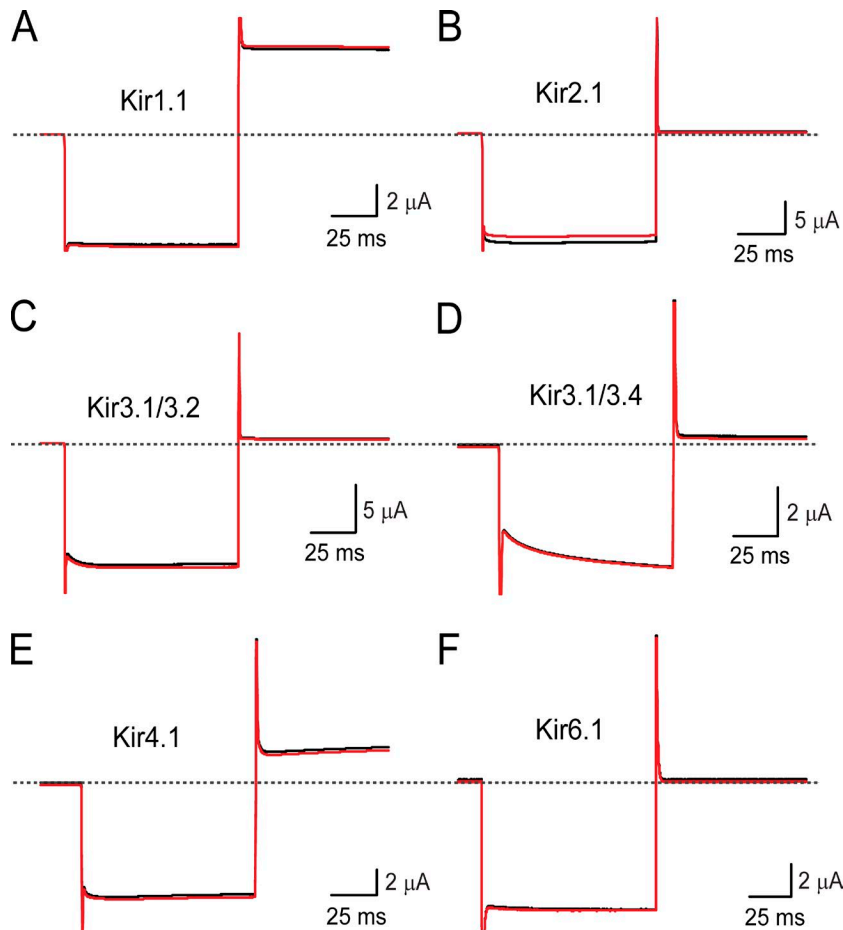


Figure 6. **Selectivity of SpTx-1 among various types of Kir channels.** (A–F) Currents of six types of Kir channels, recorded in the absence (black traces) or presence (red traces) of 250 nM synthetic SpTx-1.

an apparent  $K_d$  of 8.5 nM (Fig. 5 B). This finding indicates that the inhibitor primarily targets the pore-forming subunit Kir6.2.

To assess the selectivity of SpTx-1, we tested it against several Kir subtypes. As shown in Fig. 6, at the concentration of 250 nM, SpTx-1 had little or no detectable effects on any of these tested channels. Thus, SpTx-1 is relatively selective among the tested channels. We, by no means, imply that SpTx-1 is so selective that it would not inhibit any other untested channels.

#### Inhibition of disease-causing mutant $K_{ATP}$ channels by SpTx-1

As already mentioned, the so-called gain-of-function mutations in Kir6.2 have been found to cause PNDM. These mutations tend to lower the apparent ATP sensitivity, and the mutant channels thus carry greater  $K^+$  current in the normal range of intracellular ATP. Some of these disease-causing mutations, e.g., Q52R and V59G, only modestly lower the sulfonylurea sensitivity of the  $K_{ATP}$  current. Patients carrying such mutations have been successfully treated with sulfonylureas. However, other mutations, e.g., I296L and G334D, practically render the  $K_{ATP}$  current insensitive to sulfonylureas. Thus, patients carrying these mutations would not be treated with sulfonylureas even at very high dosages.

We tested the present inhibitor against both types of mutations. As shown in Fig. 7, SpTx-1 suppressed the currents carried by not only sulfonylurea-sensitive mutant  $K_{ATP}$  channels but also the insensitive ones. The inhibitor suppressed both mutant types with affinities comparable to that of the wild type.

## Discussion

Through screening venoms from over 200 animals, we have identified and synthesized the small protein SpTx-1 that inhibits human  $K_{ATP}$  channels with high affinity (Figs. 2, 3, and 4), which is naturally expressed in the pancreatic  $\beta$  cells. SpTx-1 suppresses, with comparable apparent  $K_d$ ,  $K^+$  current through either the channel's pore formed by four Kir6.2 subunits coexpressed with SUR1 or that formed by the Kir6.2- $\Delta$ C26 mutant subunits alone without SUR1 (Fig. 5). Thus, it inhibits the  $K_{ATP}$  channel primarily by targeting Kir6.2 rather than SUR1. Both the equilibrium and kinetic characteristics of Kir6.2 inhibition by SpTx-1 are consistent with one-to-one stoichiometry between the channel and the inhibitor (Fig. 4). SpTx-1 will be a useful tool to experimentally distinguish Kir6.2 from other channels, such as Kir6.1.

The mechanism by which nucleotides regulate  $K_{ATP}$  channels is complex (Enkvetchakul et al., 2000; Enkvetchakul and Nichols, 2003; Proks et al., 2013). Each Kir6.2 subunit contains an ATP-binding site; ATP binding there inhibits  $K_{ATP}$  current. The SUR1 subunits can bind not only MgATP but also MgADP at distinct sites (Lee et al., 2017). As the channel activity is stimulated by the binding of ADP to SUR1, it depends on the ADP and ATP ratio. The mechanism underlying sulfonylurea suppression of  $K_{ATP}$  activity is also rather complex. In the absence of ATP, a sulfonylurea molecule binds to SUR1 (Li et al., 2017; Martin et al., 2017), lowering the channel's open probability, whereas in the

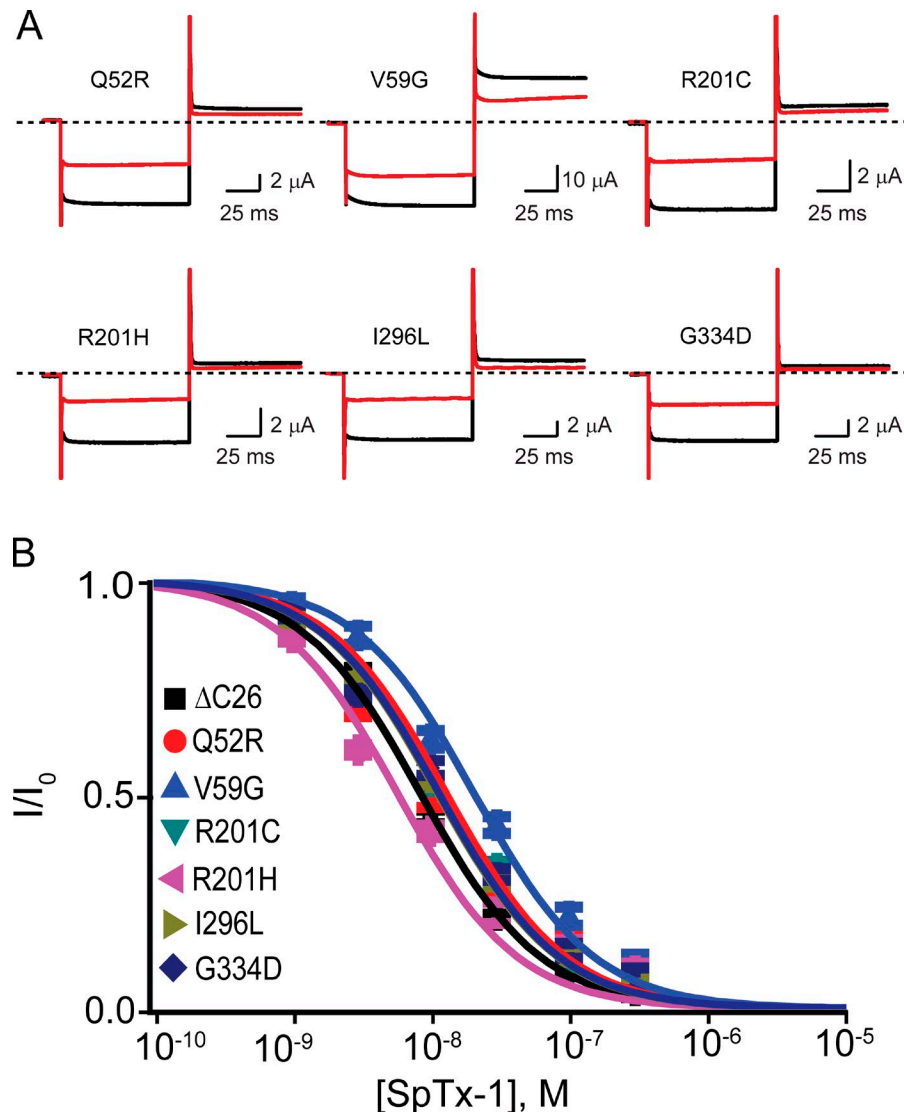


**Figure 7. SpTx-1 sensitivity of Kir6.2 containing PNDM-causing mutations. (A)** Currents of Kir6.2 with individual PNDM-causing mutations on the  $\Delta$ C26 background without (black trace) or with (red trace) the presence of 10 nM recombinant SpTx-1. **(B)** Fractions of current, recorded from the Kir6.2- $\Delta$ C26 mutant channels with or without these PNDM-causing mutations, are plotted against the concentration of SpTx-1. The  $K_d$  values determined from the curve fitting are in nM:  $8.5 \pm 0.37$  (Kir6.2- $\Delta$ C26 itself),  $13.0 \pm 3.5$  (Q52R),  $21 \pm 2$  (V59G),  $11.6 \pm 0.9$  (R201C),  $5.8 \pm 0.8$  (R201H),  $11.3 \pm 0.6$  (I296L), and  $11.6 \pm 1.2$  (G334D).  $n = 6-10$ . Data represent the mean  $\pm$  SEM.

presence of adenosine nucleotides, its binding there allosterically inhibits the ability of nucleotides to increase the channel's open probability. As such, the sulphonylurea inhibition of  $K_{ATP}$  current depends on both cell metabolism (nucleotide concentrations) and the  $K_{ATP}$  channel's nucleotide sensitivity.

Certain mutations in Kir6.2 reduce the apparent ATP sensitivity of the  $K_{ATP}$  channels in  $\beta$  cells, thus increasing the open probability of individual channels. The resulting increase in macroscopic  $K^+$  conductance hyperpolarizes the cell membrane and hampers the glucose-stimulated insulin secretion, causing PNDM. Generally, mutations that cause greater increases in  $K_{ATP}$  activity (or decreases in apparent ATP sensitivity) tend to cause more severe forms of PNDM. Most mutations in Kir6.2 increase  $K_{ATP}$  current by either directly affecting ATP binding or indirectly decreasing the effectiveness of ATP inhibition (Remedi and Koster, 2010; Nichols and Remedi, 2012; Ashcroft and Rorsman, 2013). In the latter case, mutations shift the channel's gating equilibrium toward the open state. Given that ATP preferably interacts with the closed state, a shift of gating equilibrium toward the open state lowers the apparent channel-inhibiting potency of ATP. Additionally, some mutations appear to increase  $K_{ATP}$  current

by increasing the channel's sensitivity to the stimulatory effect of magnesium-adenosine nucleotides via the SUR1 subunit.

As expected from the dependence of sulphonylurea inhibition of  $K_{ATP}$  current on both cell metabolism (nucleotide concentrations) and the channel's ATP sensitivity, these gain-of-function mutations typically reduce the effectiveness of sulphonylurea inhibition of  $K_{ATP}$  current, although the extent of reduction varies greatly among different mutations. In the cases where the reduction is not so great that the mutant channel can still be inhibited by a practically achievable sulphonylurea level, the PNDM patients tend to be treatable with high doses of sulphonylureas. Examples of Kir6.2 mutations in this category are Q52R and R201C (Proks et al., 2004). Here, we found that newly developed SpTx-1 also inhibits these mutant channels with nanomolar affinities (Fig. 7).

In some cases, mutations in Kir6.2 practically render the  $K_{ATP}$  channels insensitive to sulphonylureas. PNDM patients harboring these mutations would be insensitive to a sulphonylurea treatment. Examples of these sulphonylurea-insensitive mutations are I296L and G334D (Proks et al., 2013). We found that SpTx-1 blocks these mutant channels also with nanomolar affinities, providing an effective way to suppress gain-of-function mutant  $K_{ATP}$

channels that are insensitive to sulphonylureas (Fig. 7). We hope that SpTx-1 (and its derivatives) will serve as an effective tool to uncover new physiological and pathological roles of  $K_{ATP}$  channels, to investigate the biophysical and molecular mechanisms of Kir6.2, and to evaluate in future experiments whether Kir6.2 is an appropriate target for treating certain diabetes, such as sulphonylurea-insensitive PNDM. In the event that Kir6.2 proves to be a valid antidiabetic target, a labeled derivative of SpTx-1 can also be used to screen chemical libraries for useful small molecule-based inhibitors through competitive binding assays.

## Acknowledgments

We thank K. Ho and S. Herbert for Kir1.1 cDNA; L. Jan for Kir2.1, Kir3.1, Kir6.1, Kir6.2, and SUR1 cDNAs; H. Lester for Kir3.2 cDNA; D. Clapham for Kir3.4 cDNA; R. Buono and T. Ferraro for Kir4.1 cDNA; E.G. Peralta for M2 cDNA; G.D. Van Duyne for TEV cDNA; N. Gorman and T. Beer for the mass spectrometry analysis; and K. Stone, M. Crawford, and J. Crawford for Edman degradation sequencing and peptide synthesis.

This study was supported by the National Institute of Diabetes and Digestive and Kidney Diseases (DK109979).

The authors declare no competing financial interests.

Author contributions: All authors designed research. Y. Ramu and Y. Xu performed experiments and analyzed data. Z. Lu and Y. Ramu wrote the manuscript.

Kenton J. Swartz served as editor.

Submitted: 30 January 2018

Accepted: 27 April 2018

## References

Aguilar-Bryan, L., C.G. Nichols, S.W. Wechsler, J.P. Clement IV, A.E. Boyd III, G. González, H. Herrera-Sosa, K. Ngu, J. Bryan, and D.A. Nelson. 1995. Cloning of the beta cell high-affinity sulfonylurea receptor: A regulator of insulin secretion. *Science*. 268:423–426. <https://doi.org/10.1126/science.7716547>

American Diabetes Association. 2011. Diagnosis and classification of diabetes mellitus. *Diabetes Care*. 34(Suppl 1):S62–S69. <https://doi.org/10.2337/dc11-S062>

Ashcroft, F.M. 2005. ATP-sensitive potassium channelopathies: focus on insulin secretion. *J. Clin. Invest.* 115:2047–2058. <https://doi.org/10.1172/JCI25495>

Ashcroft, F.M., and P. Rorsman. 2012. Diabetes mellitus and the  $\beta$  cell: The last ten years. *Cell*. 148:1160–1171. <https://doi.org/10.1016/j.cell.2012.02.010>

Ashcroft, F.M., and P. Rorsman. 2013.  $K_{ATP}$  channels and islet hormone secretion: New insights and controversies. *Nat. Rev. Endocrinol.* 9:660–669. <https://doi.org/10.1038/nrendo.2013.166>

Ashcroft, F.M., D.E. Harrison, and S.J. Ashcroft. 1984. Glucose induces closure of single potassium channels in isolated rat pancreatic beta-cells. *Nature*. 312:446–448. <https://doi.org/10.1038/312446a0>

Enkvetchakul, D., and C.G. Nichols. 2003. Gating mechanism of  $K_{ATP}$  channels: function fits form. *J. Gen. Physiol.* 122:471–480. <https://doi.org/10.1085/jgp.200308878>

Enkvetchakul, D., G. Loussouarn, E. Makhina, S.L. Shyng, and C.G. Nichols. 2000. The kinetic and physical basis of  $K_{ATP}$  channel gating: Toward a unified molecular understanding. *Biophys. J.* 78:2334–2348. [https://doi.org/10.1016/S0006-3495\(00\)76779-8](https://doi.org/10.1016/S0006-3495(00)76779-8)

Gill, S.C., and P.H. von Hippel. 1989. Calculation of protein extinction coefficients from amino acid sequence data. *Anal. Biochem.* 182:319–326. [https://doi.org/10.1016/0003-2697\(89\)90602-7](https://doi.org/10.1016/0003-2697(89)90602-7)

Girard, C.A., F.T. Wunderlich, K. Shimomura, S. Collins, S. Kaizik, P. Proks, F. Abdulkader, A. Clark, V. Ball, L. Zubevici, et al. 2009. Expression of an activating mutation in the gene encoding the  $K_{ATP}$  channel subunit Kir6.2 in mouse pancreatic beta cells recapitulates neonatal diabetes. *J. Clin. Invest.* 119:80–90.

Gloyn, A.L., E.R. Pearson, J.F. Antcliff, P. Proks, G.J. Bruining, A.S. Slingerland, N. Howard, S. Srinivasan, J.M. Silva, J. Molnes, et al. 2004. Activating mutations in the gene encoding the ATP-sensitive potassium-channel subunit Kir6.2 and permanent neonatal diabetes. *N. Engl. J. Med.* 350:1838–1849. <https://doi.org/10.1056/NEJMoa032922>

Gribble, F.M., R. Ashfield, C. Ammälä, and F.M. Ashcroft. 1997. Properties of cloned ATP-sensitive  $K^+$  currents expressed in *Xenopus* oocytes. *J. Physiol.* 498:87–98. <https://doi.org/10.1113/jphysiol.1997.sp021843>

Inagaki, N., T. Gono, J.P. Clement IV, N. Namba, J. Inazawa, G. Gonzalez, L. Aguilar-Bryan, S. Seino, and J. Bryan. 1995. Reconstitution of IKATP: An inward rectifier subunit plus the sulfonylurea receptor. *Science*. 270:1166–1170. <https://doi.org/10.1126/science.270.5239.1166>

Jin, W., and Z. Lu. 1998. A novel high-affinity inhibitor for inward-rectifier  $K^+$  channels. *Biochemistry*. 37:13291–13299. <https://doi.org/10.1021/bi981178p>

Koster, J.C., B.A. Marshall, N. Ensor, J.A. Corbett, and C.G. Nichols. 2000. Targeted overactivity of beta cell  $K_{ATP}$  channels induces profound neonatal diabetes. *Cell*. 100:645–654. [https://doi.org/10.1016/S0092-8674\(00\)80701-1](https://doi.org/10.1016/S0092-8674(00)80701-1)

Lee, K.P.K., J. Chen, and R. MacKinnon. 2017. Molecular structure of human  $K_{ATP}$  in complex with ATP and ADP. *Elife*. 6:e32481. <https://doi.org/10.7554/eLife.32481>

Li, N., J.X. Wu, D. Ding, J. Cheng, N. Gao, and L. Chen. 2017. Structure of a Pancreatic ATP-Sensitive Potassium Channel. *Cell*. 168:101–110.e10. <https://doi.org/10.1016/j.cell.2016.12.028>

Martin, G.M., B. Kandasamy, F. DiMaio, C. Yoshioka, and S.L. Shyng. 2017. Anti-diabetic drug binding site in a mammalian  $K_{ATP}$  channel revealed by Cryo-EM. *Elife*. 6:e31054. <https://doi.org/10.7554/eLife.31054>

Miki, T., K. Nagashima, F. Tashiro, K. Kotake, H. Yoshitomi, A. Tamamoto, T. Gono, T. Iwanaga, J. Miyazaki, and S. Seino. 1998. Defective insulin secretion and enhanced insulin action in  $K_{ATP}$  channel-deficient mice. *Proc. Natl. Acad. Sci. USA*. 95:10402–10406. <https://doi.org/10.1073/pnas.95.18.10402>

Nichols, C.G. 2006.  $K_{ATP}$  channels as molecular sensors of cellular metabolism. *Nature*. 440:470–476. <https://doi.org/10.1038/nature04711>

Nichols, C.G., and M.S. Remedi. 2012. The diabetic  $\beta$ -cell: Hyperstimulated vs. hyperexcited. *Diabetes Obes. Metab.* 14(Suppl 3):129–135. <https://doi.org/10.1111/j.1463-1326.2012.01655.x>

Noma, A. 1983. ATP-regulated  $K^+$  channels in cardiac muscle. *Nature*. 305:147–148. <https://doi.org/10.1038/305147a0>

Pearson, E.R., I. Flechtner, P.R. Njolstad, M.T. Malecki, S.E. Flanagan, B. Larkin, F.M. Ashcroft, I. Klimes, E. Codner, V. Iotova, et al. Neonatal Diabetes International Collaborative Group. 2006. Switching from insulin to oral sulphonylureas in patients with diabetes due to Kir6.2 mutations. *N. Engl. J. Med.* 355:467–477. <https://doi.org/10.1056/NEJMoa061759>

Proks, P., J.F. Antcliff, J. Lippiat, A.L. Gloyn, A.T. Hattersley, and F.M. Ashcroft. 2004. Molecular basis of Kir6.2 mutations associated with neonatal diabetes or neonatal diabetes plus neurological features. *Proc. Natl. Acad. Sci. USA*. 101:17539–17544. <https://doi.org/10.1073/pnas.0404756101>

Proks, P., H. de Wet, and F.M. Ashcroft. 2013. Molecular mechanism of sulphonylurea block of  $K_{ATP}$  channels carrying mutations that impair ATP inhibition and cause neonatal diabetes. *Diabetes*. 62:3909–3919. <https://doi.org/10.2337/db13-0531>

Remedi, M.S., and J.C. Koster. 2010.  $K_{ATP}$  channelopathies in the pancreas. *Pflugers Arch.* 460:307–320. <https://doi.org/10.1007/s00424-009-0756-x>

Remedi, M.S., S.E. Agapova, A.K. Vyas, P.W. Hruz, and C.G. Nichols. 2011. Acute sulphonylurea therapy at disease onset can cause permanent remission of  $K_{ATP}$ -induced diabetes. *Diabetes*. 60:2515–2522. <https://doi.org/10.2337/db11-0538>

Rorsman, P., and G. Trube. 1985. Glucose dependent  $K^+$ -channels in pancreatic beta-cells are regulated by intracellular ATP. *Pflugers Arch.* 405:305–309. <https://doi.org/10.1007/BF00595682>

Tucker, S.J., F.M. Gribble, C. Zhao, S. Trapp, and F.M. Ashcroft. 1997. Truncation of Kir6.2 produces ATP-sensitive  $K^+$  channels in the absence of the sulphonylurea receptor. *Nature*. 387:179–183. <https://doi.org/10.1038/387179a0>

Zhang, H., T.P. Flagg, and C.G. Nichols. 2010. Cardiac sarcolemmal  $K_{ATP}$  channels: Latest twists in a queuing tale! *J. Mol. Cell. Cardiol.* 48:71–75. <https://doi.org/10.1016/j.jmcc.2009.07.002>